Supplemental Figures

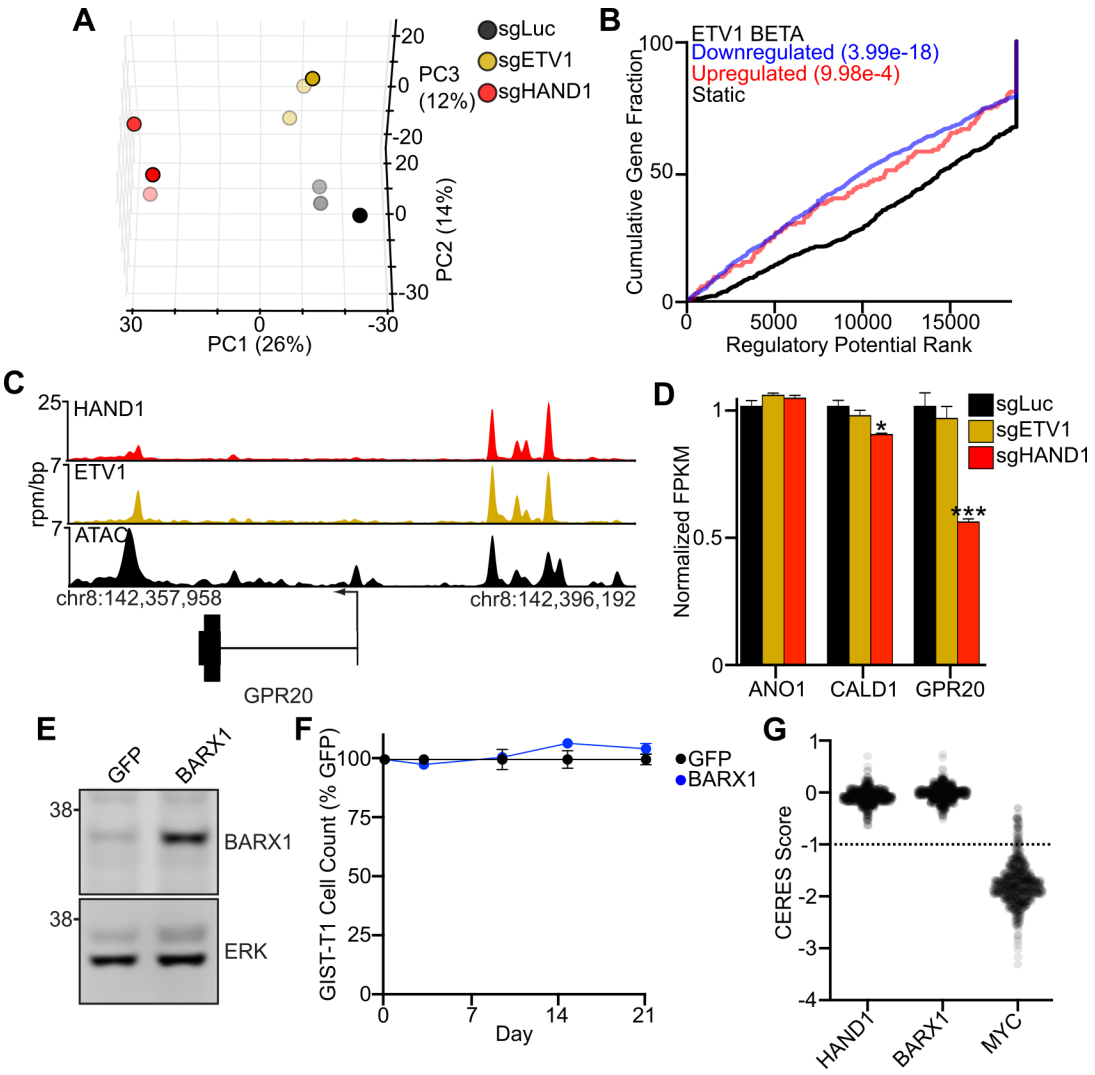

Figure S1. Effects of GIST TF manipulation *in vitro*. A, PCA of RNA-seq data from GIST-T1 cells treated for 5 days with the indicated sgRNAs (*n*=3 per group). **B,** BETA integration of ETV1 ChIP-seq and differential gene expression for sgETV1 and sgLuc comparisons. **C,** ChIP-seq tracks for HAND1 and ETV1 and ATAC peaks at the *GPR20* locus. **D,** Expression of GIST biomarkers in cells treated with sgHAND1, sgETV1 or sgLuc as control. Data were analyzed by one-way ANOVA with Dunnett's multiple comparison test (*n*=3; compared to sgLuc; *,*P*<0.05; ***,*P*<0.001). **E,** BARX1 overexpression in GIST-T1 demonstrated by BARX1 Western blot, with total ERK levels shown as loading control. **F,** Growth over time assay following stable expression of BARX1 or GFP as control. Cell count is normalized to GFP control (*n*=5 per construct). **G,** CERES gene dependency scores for HAND1 (*n*=789), BARX1 (*n*=789) or MYC (*n*=777) as comparator across cell lines profiled in the DepMap portal. The horizontal line at -1 indicates the threshold for considering a gene essential in a given cell line. No GIST cell lines have yet been included in the DepMap portal.

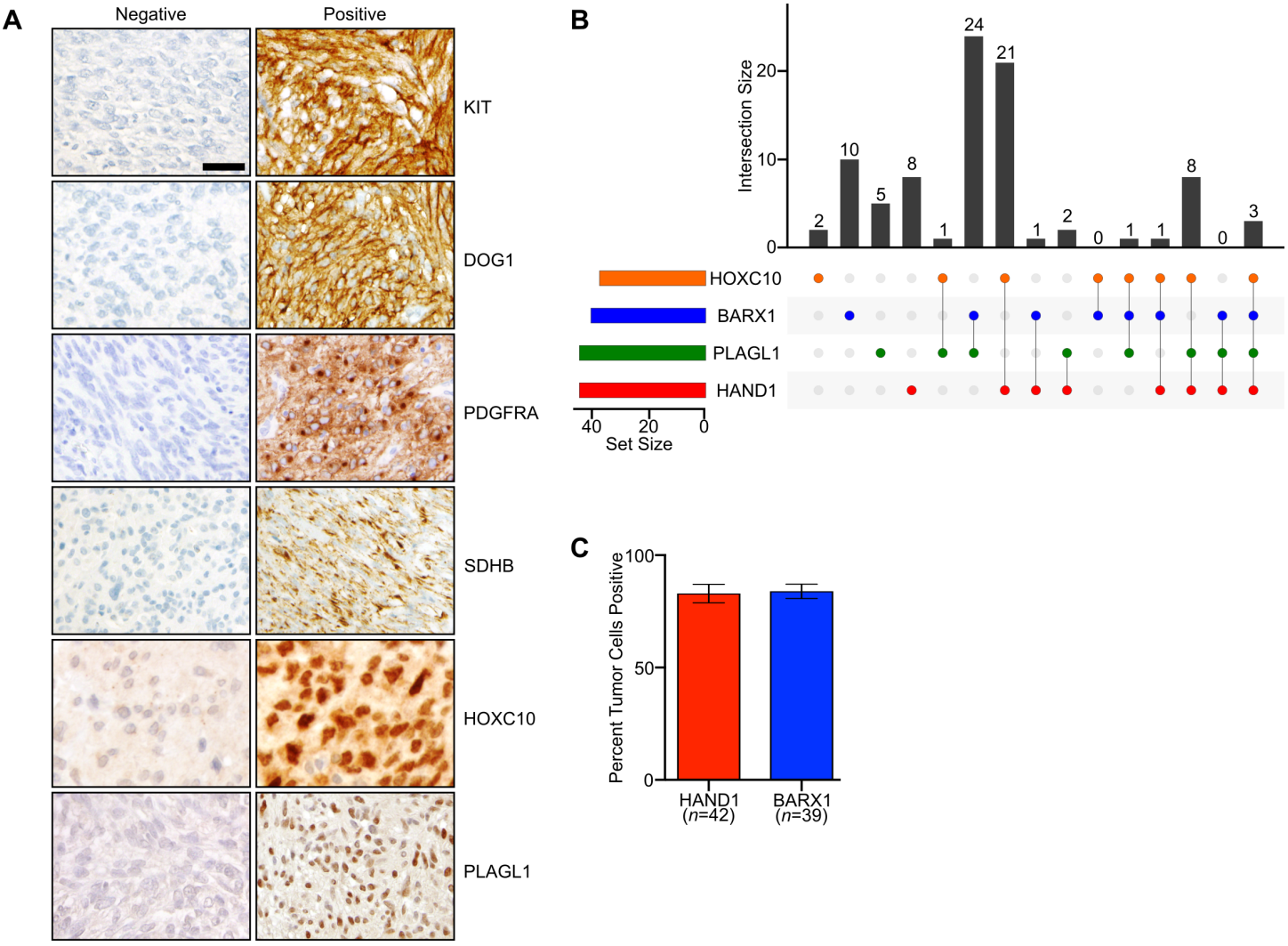

Figure S2. Expression patterns of GIST biomarkers and TFs. A, KIT, DOG1, PDGFRA, SDHB, HOXC10 and PLAGL1 IHC, with examples of negative and positive samples shown. DOG1 and KIT exhibit a membranous expression pattern, PDGFRA a peri-nuclear Golgi or dot-like expression pattern in PDGFRA-mutant GIST, and nuclear localization of TFs (scale bar, 20 μm). **B,** Upset plot showing co-expression relationships of HAND1, HOXC10, BARX1 and PLAGL1. **C,** Percentage of tumor cells positive by IHC for HAND1 (*n*=42) or BARX1 (*n*=39) by blinded expert pathology review in tumors expressing either marker.

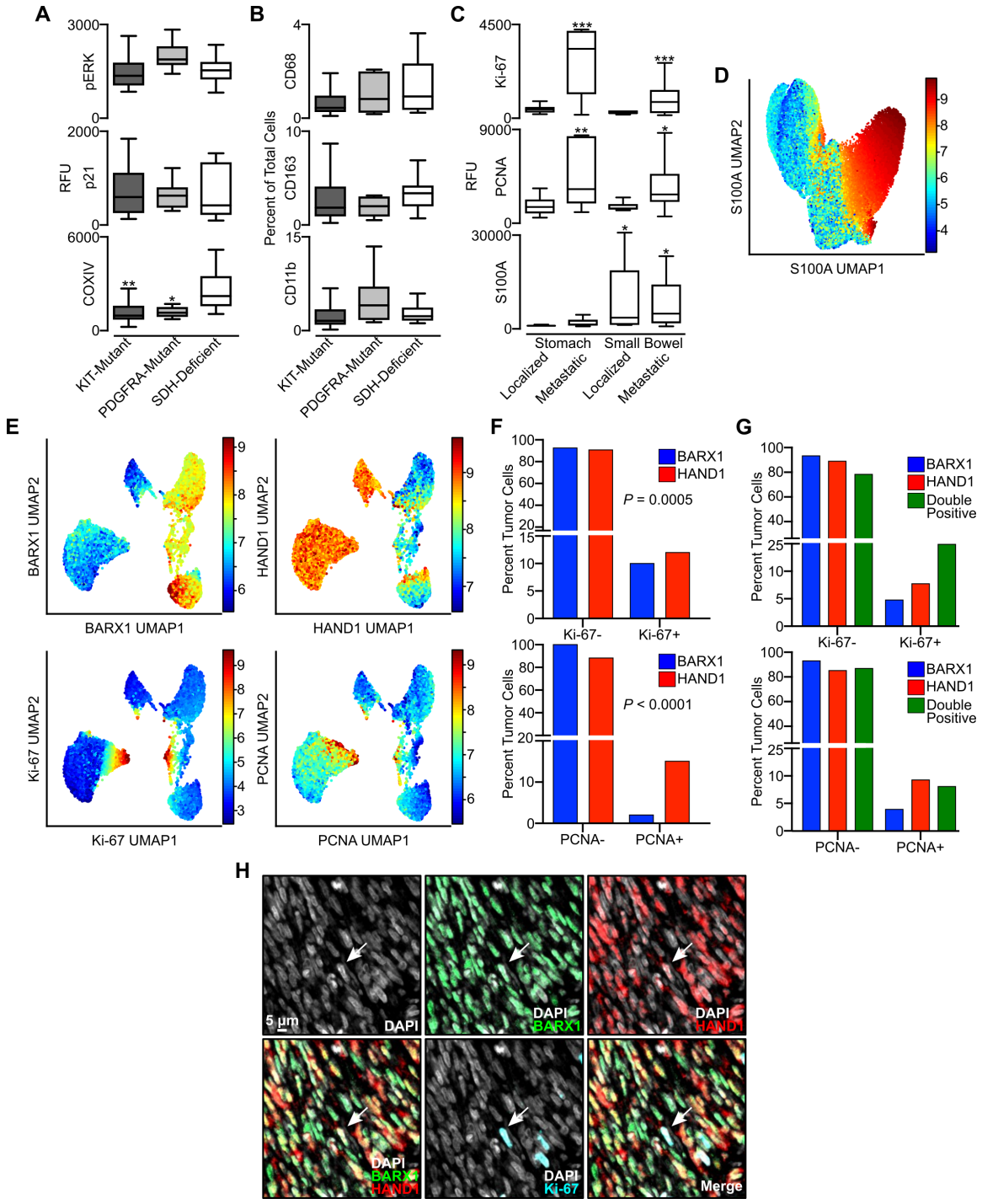

Figure S3. Tissue level and single cell analysis of multiplexed CyCIF imaging. A, Relative intensity of signal in whole tissue of phospho-ERK, p21 and COXIV in KIT-mutant (*n*=65), PDGFRA-mutant (*n*=10), and SDH-deficient (*n*=12) GIST. Data were analyzed by one-way ANOVA with Tukey's multiple comparison test (compared to SDH-deficient GIST; *,*P*<0.05; **,*P*<0.0015). **B,** Percent of total cells in whole tissues expressing CD68, CD163 and CD11b in KIT-mutant (*n*=65), PDGFRA-mutant (*n*=10), and SDH-deficient (*n*=12) GIST. **C,** Relative signal of Ki-67, PCNA and S100A in KIT-mutant GIST stratified by anatomic origin and localized versus metastatic state. Data were analyzed by one-way ANOVA with Tukey's multiple comparison test (compared to localized gastric GIST; *,*P*<0.05; **,*P*<0.001; ***,*P*<0.0001). **D,** UMAP of all tumor samples for single tumor cells (87 tumors, *n*=156,036 cells), defined by the expression of HAND1 and/or BARX1, with heatmap showing S100A signal. **E,** UMAP with single cell analysis of tumors expressing both HAND1 and BARX1 by IHC (5 tumors, *n*=11,658 cells) with heatmaps showing HAND1, BARX1, Ki-67, and PCNA $\log_2$ RFU. **F,** Percent of tumor cells from IHC double-positive samples that were negative or positive for Ki-67 (upper panel) or PCNA (lower panel) stratified by BARX1 (blue, *n*=4,871) or HAND1 (red, *n*=6,350) expression.

Data were analyzed by Fisher's exact test with *P* value indicated. **G,** Percent of all tumor cells that were negative or positive for Ki-67 (upper panel) or PCNA (lower panel) stratified by BARX1 expression (blue, *n*=65,340), HAND1 expression (red, *n*=81,501), or double positive cells expressing both BARX1 and HAND1 (green, *n*=9,195). **H,** Image showing signal for DAPI (white), BARX1 (green), HAND1 (red) and Ki-67 (blue) in a tumor positive for both HAND1 and BARX1 by IHC (scale bar, 5 μm).

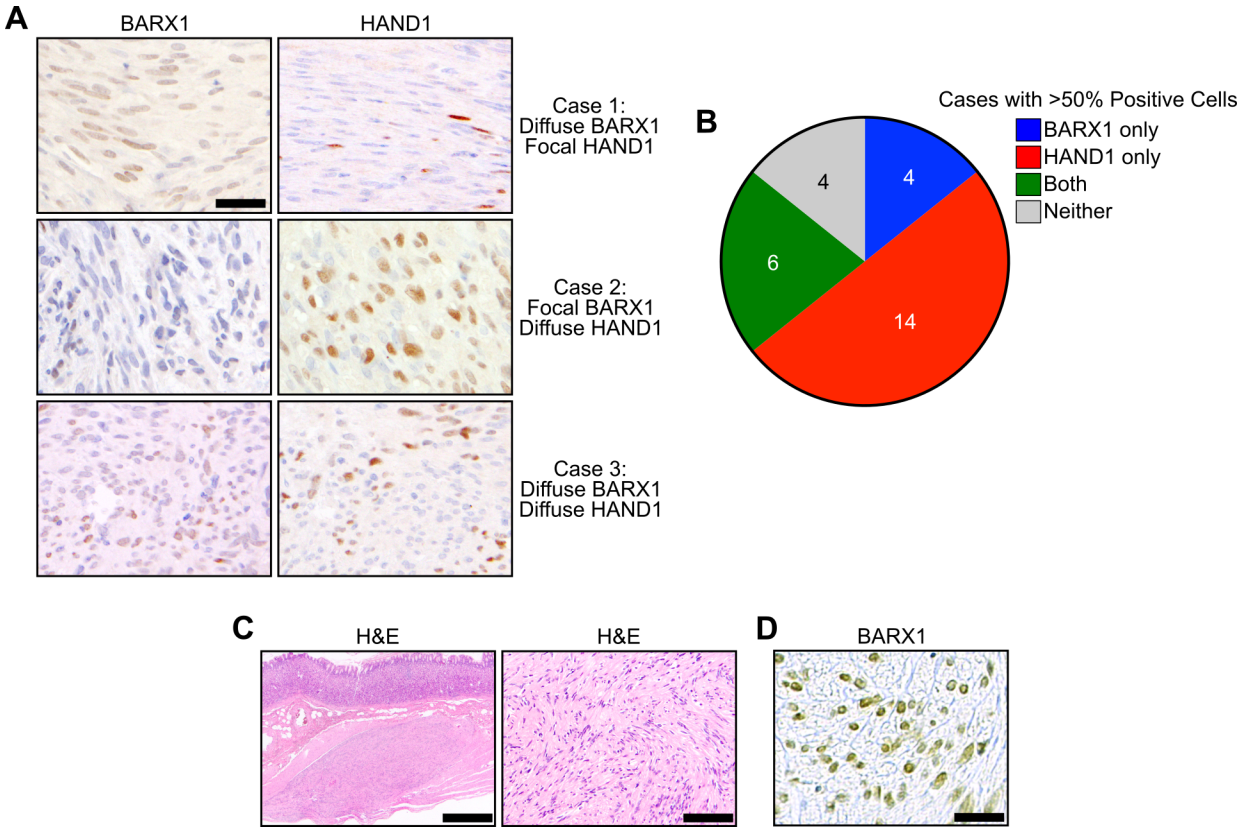

Figure S4. GIST samples with heterogeneous BARX1 and HAND1 expression and BARX1 expression in micro-GIST. A, Individual cases with diffuse BARX1 and focal HAND1 (top panels, scale bar indicates 20 μm), focal BARX1 and diffuse HAND1 (middle panels), and diffuse BARX1 and diffuse HAND1 (lower panels). **B,** Pie chart showing the distribution double positive cases categorized by one, both or neither TF being expressed in >50% of tumor cells. **C,** H&E of micro-GIST (left panel scale bar 500 μm; right panel 50 μm). **D,** BARX1 IHC of micro-GIST (scale bar, 20 μm).

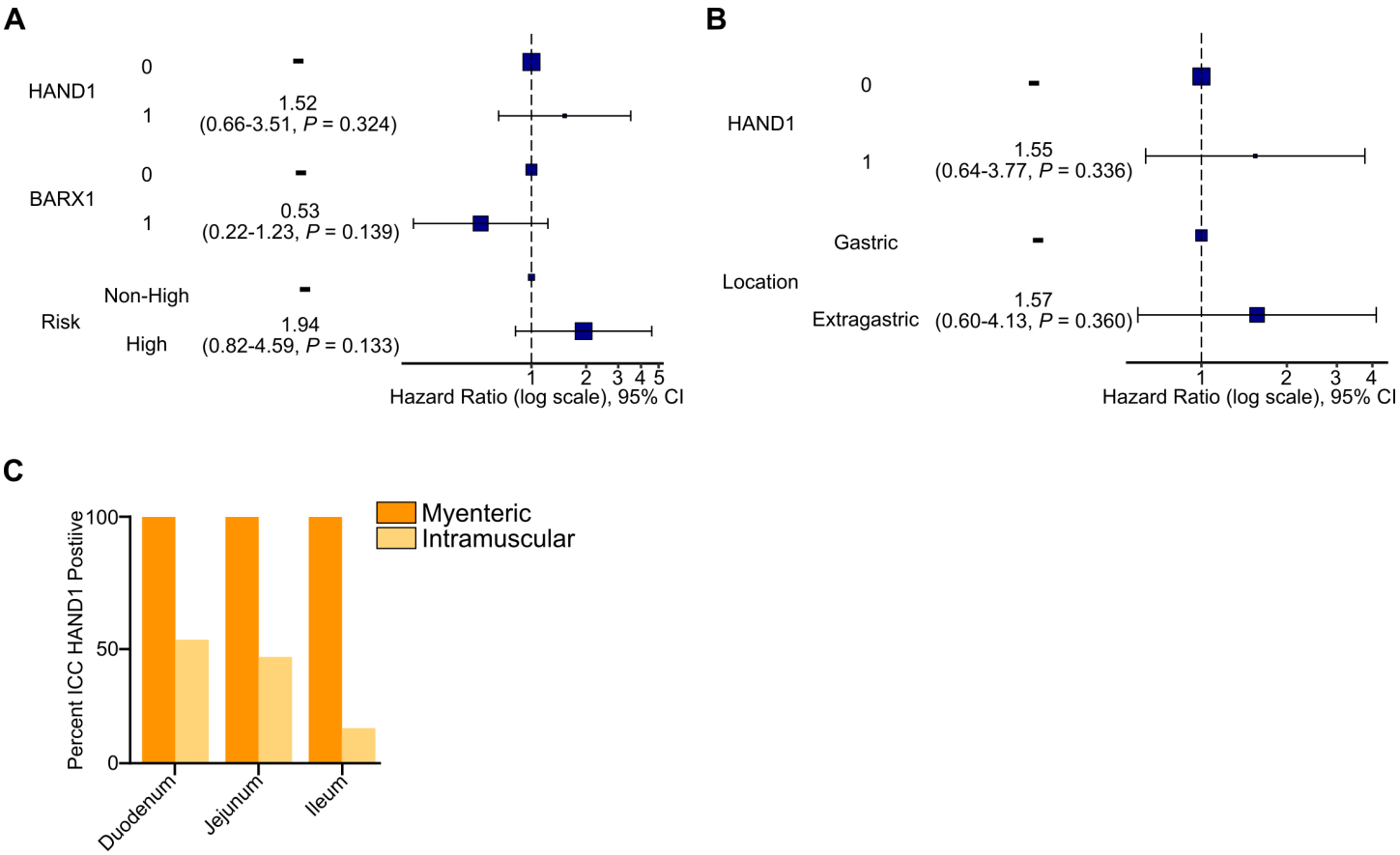

Figure S5. GIST Multivariate Analysis and HAND1 in ICCs of the small intestine. A, Hazard-ratio plot with corresponding 95% confidence intervals for a multivariable Cox proportional hazards model for relapse-free survival as a function of HAND1 status (ref: HAND1-), BARX1 status (ref: BARX1-) and Risk status (ref: Non-High Risk). **B,** Hazard-ratio plot with corresponding 95% confidence intervals for a multivariable Cox proportional hazards model for relapse-free survival as a function of HAND1 status (ref: HAND1-) and tumor location (ref: gastric). **C,** Within the small intestine, percentage of whole slides with ICC that were positive for HAND1 at myenteric or intramuscular sites in the duodenum (*n*=14), jejunum (*n*=7) or ileum (*n*=7).

Table S1. GIST RNA-seq Cohort

Table S2. CyCIF Antibodies

Table S3. CyCIF Proliferation Percentages. Individual cells expressing HAND1, BARX1 or positive for both TFs in all samples (*n*=87), localized gastric tumors (*n*=15) and GIST tumors double-positive by IHC for both TFs (*n*=5) stratified by Ki-67 and PCNA expression.

Table S4. GIST Immunohistochemistry Cohort. Summary of all samples (*n*=437) with available information including gender, age at diagnosis, primary tumor site, GIST oncogene subtype and mutated exon. The cohort is stratified by HAND1 and BARX1 expression, with summary statistics shown.

Table S5: Cases of BARX1-/HAND1- GIST

Table S6: Cases of BARX1+/HAND1- Extragastric GIST